

## Phonons in GaP quantum dots

Huaxiang Fu, V. Ozoliņš, and Alex Zunger  
*National Renewable Energy Laboratory, Golden, Colorado 80401*  
~Received 10 August 1998!

The phonon structure of GaP quantum dots is studied using an atomistic potential model. The dot eigenmodes are obtained from a direct diagonalization of the dynamical matrix and classified using an efficient dual-space analysis method. Our calculations provide a theoretical explanation for several experimental observations. ~1! Depending on the spatial localization, the phonon modes of dots are either dot-interior ~bulklike! or surfacelike. ~2! The frequencies of the dot-interior modes can be qualitatively described by the “truncated crystal method” using a single branch and a single wave vector of the bulk-phonon dispersion. In contrast, the surface modes cannot be described by this model. ~3! The dot-interior modes have a dominant bulk parentage from a specific part of the Brillouin zone, while the surface modes do not. ~4! The frequencies of the bulklike G-derived longitudinal optical ~LO! and transverse optical ~TO! phonon modes are found to decrease with decreasing dot size. This decrease reflects the downward dispersion of the bulk optical-phonon branches away from the G point. ~5! The surface modes located between the bulk TO- and LO-phonon bands have a significant bulk G character, and are thus Raman detectable. ~6! The dot-interior modes exhibit only a slight LO/TO mode mixing, while the surfacelike modes show a strong mode mixing. ©0163-1829-99

dot size. This is consistent with experiments.<sup>10</sup> Unlike the case in PbS dots,<sup>1</sup> we find no significant LO/TO mixing for the bulklike modes in GaP dots.

The surfacelike modes are localized at the periphery of the dot, and their eigenvectors are superpositions of many bulk-phonon states from different bands and different points of the Brillouin zone. The surfacelike modes located between the bulk LO- and TO-phonon bands have a significant bulk-G character and, thus, may be Raman active. In contrast to the bulklike modes, these surfacelike modes exhibit significant LO/TO mixing.

## II. THEORETICAL METHODS

### A. Phonon frequencies and eigenstates: Bulk and dots

The atom-atom force field  $U(\mathbf{r}_i) \approx U_{\text{SR}} + U_{\text{LR}}$  used here includes a short-range part  $U_{\text{SR}}$ , which describes the covalent bonding, and a long-range part  $U_{\text{LR}}$ , which describes the Coulomb interaction between point-charged ions. For atom  $i$  bonded tetrahedrally to atoms  $j$  and  $k$ , the short-range interaction is

$$U_{\text{SR}}(\mathbf{r}_i) \approx \frac{1}{a_0^2} \left( \sum_{j,k} a_{ij} \mathbf{r}_{ij}^2 + \sum_{j,k} b_{jik} \mathbf{r}_{ij} \cdot \mathbf{r}_{ik} + \sum_{j,k} g_{jik} \mathbf{r}_{ij}^2 \right)$$

$$R_1^2 \propto \left( \int_{r \in \mathcal{B}_1} |Q_1^{r \sim i}|^2 |\mathbf{r}_i - \mathbf{r}_c|^2, \quad \sim 8!$$

where  $\mathbf{r}_c$  is the dot center.  $R_1$  tells us in what part of the dot is the eigenmode  $l$  localized, distinguishing modes that are localized inside the dot ~“bulklike modes”! from those localized at the periphery of the dot ~“surfcelike modes”!.

In reciprocal space we use the projection approach to establish the relation between the dot modes and the bulk modes.<sup>25</sup> We first expand the dot displacements  $\mathbf{u}_1^{\text{dot}}$  in the bulk states  $\mathbf{u}_{n\mathbf{k}}^{\text{bulk}}$  of branch  $n$  and wave vector  $\mathbf{k}$ :

$$\mathbf{u}_1^{\text{dot}} \sim i! \int_{\mathcal{B}} d\mathbf{k} C_{n\mathbf{k}}^{-1} \mathbf{u}_{n\mathbf{k}}^{\text{bulk}} \sim i!. \quad \sim 9!$$

The projection coefficients  $C_{n\mathbf{k}}^{(1)}$  are calculated using the orthogonality of  $\mathbf{u}_{n\mathbf{k}}^{\text{bulk}}$ . We define the *Brillouin-zone parentage*  $P_1(k)$  of a dot mode  $l$  as the contribution of the bulk eigenmodes with the wavevector length  $k$  in forming this dot mode:

$$P_1 \sim k! \int d\mathbf{k} d|\mathbf{k}| \mathcal{Z} k! \left( |C_{n\mathbf{k}}^{-1}|^2. \quad \sim 10!$$

This quantity tells us which part of the bulk Brillouin zone ~BZ! contributes to a given dot eigenmode. We also define the *bulk-G parentage*  $T_1(n, K_{\text{cut}})$  measuring the extent to which the dot eigenmode is derived from the bulk states near  $\Gamma$ :

$$T_1 \sim n, K_{\text{cut}}! \int_0^K$$

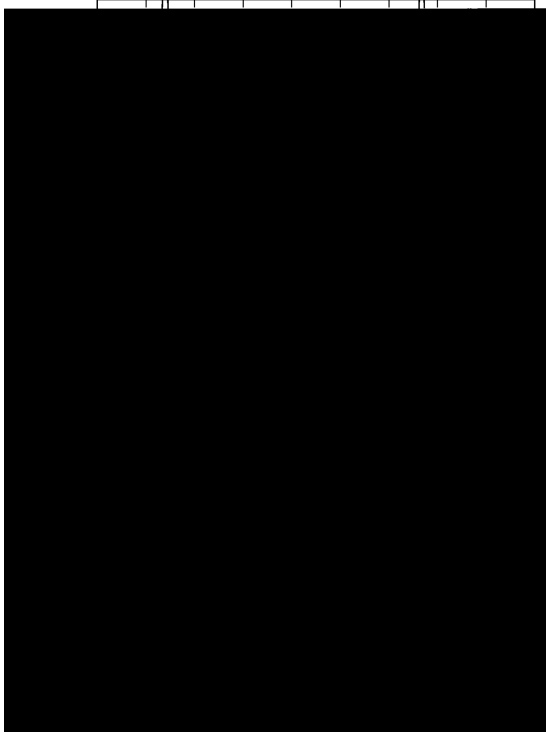


FIG. 2. -a! Density of phonon states for GaP quantum dots of

Fig. 2. Region I ( $n^2 \approx 60\text{--}90 \text{ THz}^2$ ) is the phonon gap between the bulk acoustic and optical modes, and region II ( $n^2 \approx 120\text{--}130 \text{ THz}^2$ ) is the phonon gap between the bulk TO and LO modes. We will see later from the ‘‘localization radii’’ @Fig. 2-b!# that these ‘‘gap modes’’ are localized on the dot surface.

-iii! Although the ‘‘gap modes’’ exist even in the very large dots ~with several thousands of atoms!, their peak intensities relative to the bulklike modes decrease significantly with increasing dot size.

### C. Mode analysis using the dual-space approach

The ‘‘localization radii’’ @see Eq. ~8!# for the dot with diameter  $D \approx 32.5 \text{ \AA}$  are shown in Fig. 2-b!. Comparison with the phonon DOS in Fig. 2-a! shows the following features.

-i! The gap modes in regions I and II have their mode centers close to the dot’s surface @Fig. 2-b!#, thus being ‘‘surfacerlike modes.’’

-ii! The dot modes that correspond to the sharp peaks of the bulk DOS have their localization radii in the dot’s interior, thus being ‘‘bulklike’’ ~dot-interior! modes. Our ‘‘Brillouin-zone parentage’’ analysis and the frequencies of the dot modes indicate that the modes at  $n^2 \approx 9, 40, 95, 113,$  and  $138 \text{ THz}^2$  in Fig. 2-b! are derived from the bulk TA(X)

~TA modes near the X point!, LA(L), TO(S) ~TO modes along the @110# direction!, TO(X), and LO(S) modes, respectively. These dot-interior modes are clearly separated from the surface modes.

-iii! The dot modes with intermediate localization radii ~around  $11 \text{ \AA}$  in Fig. 2! have their vibrational amplitudes both inside the dots and near the dot surface.

-iv! We find that the distributions of localization radii  $R_1$  vs  $n_1$  for different dot sizes contain similar features @compare Fig. 2-b! with Fig. 6 below, showing the localization radii of a much smaller dot#. This surprising ‘‘self-similarity’’ exists for both the dot-interior modes and the surfacerlike modes, and it holds to the smallest dot size considered.

To study the evolution of an individual dot mode with the size  $D$ , we have to identify the same phonon mode in different dots. We are particularly interested in the dot modes that derive from the bulk G states, since such modes play an important role in Raman scattering. We use for this purpose the ‘‘bulk-G parentage’’  $T_1(n, K_{\text{cut}})$  defined in Eq. ~11!. Figure 3-a! shows the bulk-G LO character and Fig. 3-b! gives the bulk-G TO character for the  $D \approx 32.5 \text{ \AA}$  dot phonons with frequencies above  $10 \text{ THz}$ . We see in Fig. 3-a! that a single dot mode @labeled LO(G)# originates predominantly from the bulk LO phonon near G, and another dot mode @labeled TO(G)# originates predominantly from the bulk-TO phonon near G. Between these TO(G)- and LO(G)-like modes there exist some surface modes @denoted as spin orbit ~SO! in Fig. 3, see Fig. 2-b! for their localization radii#, which have con-

tributions from both bulk TO- and LO-phonon bands. The fact that the surface modes in Fig. 3 have sizable contributions from bulk  $\mathbf{k}$  points near  $\mathbf{G}$  implies that these modes might be Raman active. Indeed, in a micro-Raman scattering study of porous GaP nanocrystallites, Tiginyanu *et al.*<sup>10</sup> observed a small peak between sharp bulk derived LO- and TO-phonon peaks. They suggested that the origin of this peak is due to the dot surface—a suggestion that is supported by our theoretical result.

#### D. Evolution of mode frequencies with dot size

Once the character of the dot modes is identified for different dot sizes (Fig. 3), we can trace the size dependence of the frequencies of these modes (Fig. 4). In order to facilitate the understanding of the evolution of phonon frequency with the dot size, we choose four special modes: the bulk-derived LO( $\mathbf{G}$ ) and TO( $\mathbf{G}$ ), the  $\mathbf{G}$ -derived acoustic mode  $A(\mathbf{G})$ , which is the dot's mode of the lowest-acoustic frequency, and the  $X$ -derived longitudinal acoustic mode LA( $X$ ), which is the dot's mode of the highest-acoustic frequency. The  $\mathbf{G}$  character of the  $A(\mathbf{G})$  mode and the  $X$  character of the LA( $X$ ) mode can be seen from their Brillouin-zone parentages (see Fig. 5 below). These four modes are all dot-interior states according to their localization radii. We see from Fig. 4 that both the TO( $\mathbf{G}$ ) and LO( $\mathbf{G}$ ) modes shift *down* in frequency with decreasing dot size. This is consistent with the experimental measurements<sup>10</sup> where both LO- and TO-phonon Raman peaks were found to shift to lower frequencies with increasing anodization current (i.e., decreasing dot

size) in porous GaP nanocrystallites. The frequency of the acoustic mode  $A(\mathbf{G})$  *increases* as the dot size decreases.

Analytically fitting the calculated results gives

$$Dn \approx \begin{cases} 8.84/D^{1.04} & @A\text{-}\mathbf{G}\text{!}\# \\ 274.75/D^{2.04} & @TO\text{-}\mathbf{G}\text{!}\# \\ 2392.77/D^{2.32} & @LO\text{-}\mathbf{G}\text{!}\# \\ 2181.52/D^{1.84} & @LA\text{-}\mathbf{X}\text{!}\#, \end{cases} \quad \sim 13!$$

where  $Dn$  is in units of THz and  $D$  is in units of  $\text{\AA}$ . The fitted results are shown in Fig. 4 as solid lines. We see that, while the frequency shift of the  $A(\mathbf{G})$  mode is almost inversely linear with the dot size, it is close to  $1/D^2$  for the other three modes.

To understand this frequency shift with the dot size, we recall from Eq. (9) that, in general, the frequency of a *bulk-like* mode can be expressed as a linear combination of the bulk-phonon frequencies:

$$\omega_{\mathbf{k}}^{\text{dot}} \approx \sum_{n,\mathbf{k}} c_n \omega_{n,\mathbf{k}}^{\text{bulk}}$$

TABLE III. Bulk-band parentage  $A_1(n)$  @Eq. ~12!# of bulk-phonon bands ( $n \in 1, \dots, 6$ ) in forming the  $A(G)$ ,  $LA(X)$ ,  $TO(G)$ ,  $LO(G)$ , and  $SO$  modes of the  $D \approx 32.5 \text{ \AA}$  dot.

Dot mode l	Contribution $A_1(n)$ -in %! of bulk band $n$ to dot mode l			
	$n \in 1$ -TA!	$n \in 3$ -LA!	$n \in 4$ -TO!	$n \in 6$ -LO!
$A(G)$	<b>86.5</b>	3.9	8.1	1.5
$LA(X)$	0.8	<b>91.3</b>	4.1	3.9
$TO(G)$	5.4	0.5	<b>87.7</b>	6.4
$LO(G)$	0.1	3.6	0.9	<b>95.4</b>
$SO$	1.9	4.1	<b>31.5</b>	<b>62.5</b>

$$n_1^{\text{dot}}, n_{nk}^{\text{bulk}} \quad \sim 15!$$

We use the ‘‘Brillouin-zone parentage’’  $P_1(k)$  to answer this. Figure 5 shows, for the  $D \approx 32.5 \text{ \AA}$  dot, the Brillouin-zone parentages of the bulklike  $A(G)$ ,  $TO(G)$ ,  $LO(G)$ , and  $LA(X)$  modes with frequencies  $n^2 \approx 0.046, 119.2, 140.7$ , and  $51.1 \text{ THz}^2$ , respectively.

We see from Fig. 5 that the above considered bulklike modes all have a dominant BZ parentage peak around their bulk origins @.g.,  $A(G)$ ,  $TO(G)$ ,  $LO(G)$  near  $G$ , and  $LA(X)$  near  $X$ , i.e., for the bulklike dot modes there exists a  $\mathbf{k}^*$  that satisfies Eq. ~15!. For the  $G$ -derived  $A(G)$ ,  $TO(G)$ , and  $LO(G)$  modes, the peak positions of the Brillouin-zone parentages are located near  $|\mathbf{k}^*| \approx 2p/D$ . In fact, this  $\mathbf{k}^*$  has been used<sup>33</sup> in the ‘‘truncated crystal’’ method to estimate the electronic-orbital energy in dots from the bulk-band structure using Eq. ~15!. In the truncated-crystal method one seeks a wave vector  $\mathbf{k}^*$  for which the envelope function vanishes at the dot boundary. For spherical dots the smallest  $k^*$  that satisfies this boundary condition is  $2p/D$ . This approach then relates the *bulk dispersion*  $n_{nk}$  to the frequency  $n_1$  in dots. The smaller the dot, the further does  $k^* \propto 1/D$  move away from the  $G$  point. Thus, the slope of the bulk dispersion away from  $G$  determines, in this model, the size dependence of the frequency of the dot’s mode. Since the frequency of the bulk GaP optical phonons -Fig. 1! decreases when  $\mathbf{k}$  departs from the  $G$  point, the frequencies of the dot’s  $TO(G)$  and  $LO(G)$  modes should exhibit a *redshift* relative to their bulk values. This expectation is confirmed by our results obtained from the direct diagonalization of the dynamical matrix -Fig. 4!. The scaling exponent  $t$  of  $1/D^t$  in Eq. ~13! can also be qualitatively understood from a TC-type argument: since the frequencies of the bulk acoustic-phonon branches near  $G$  are linear functions of the wave vector  $n \propto k$ , and since  $k^* \propto 1/D$ , we obtain that  $dn \propto 1/D$  -i.e.,  $t \approx 1$ ), as indeed given by Eq. ~13! for the  $A(G)$  mode. The bulk-phonon dispersion relations of the LO- and TO-phonon modes at  $G$  and of the LA-phonon mode at  $X$  are parabolic and, thus, lead to  $dn \propto 1/D^2$ , i.e.,  $t \approx 2$  in Eq. ~13!. More quantitatively, Table II compares the frequencies of the bulklike dot modes, as obtained from direct calculations, with those obtained from Eq. ~15!. We see that the two methods give the same trend of the frequency change with the dot size, and that they give quantitatively accurate results for the bulklike LO- and TO-derived modes. However, for the  $A(G)$  dot-phonon mode, the frequencies obtained from the two methods are quite different. This is probably due to the surface effect, which causes this mode to have a large localiza-

tion radius @.g.,  $R_1 \approx 12 \text{ \AA}$  in Fig. 2-b!# and, therefore, destroys the conditions for the applicability of the truncated-crystal model.

Since the surfacelike modes are localized in real space on the dot surface and, therefore, contain contributions from the bulk GaP modes all over the Brillouin zone, there is not a single  $\mathbf{k}^*$  to be used in Eq. ~15! to describe their frequencies. This property of the surface modes is illustrated in Fig. 5, which shows, for comparison with the bulklike  $A(G)$ ,  $LO(G)$ ,  $TO(G)$ , and  $LA(X)$  modes, the Brillouin-zone parentage of a surfacelike optical -SO! mode with  $n^2 \approx 126.6 \text{ THz}^2$  for the  $D \approx 32.5 \text{ \AA}$  dot. We see from Fig. 5 that the surfacelike mode is delocalized in reciprocal space.



FIG. 6. ‘‘Bulk-band parentage’’  $A_1(n)$  @Eq. ~12!# of -a!  $n \in 6$  -bulk LO-phonon band! and -b!  $n \in 4$  -bulk TO-phonon bands! in forming dot modes with frequency  $n^2 \approx 40 \text{ THz}^2$ . The results for the  $D \approx 22.2 \text{ \AA}$  dot are shown. The shaded areas indicate the modes that have a sizable LO/TO mode mixing. Panel -c! shows the localization radii of the dot modes in order to facilitate the comparison.

### E. Mode mixing

An interesting possibility is the LO/TO mode mixing of the phonon modes in quantum dots, which can be induced by the lack of translational symmetry in dots. Table III gives the “bulk-band parentage” of Eq. 12 of the five dot modes shown in Fig. 5 for the  $D = 32.5 \text{ \AA}$  quantum dot. We see that in this relatively large dot there is no significant mode mixing for the bulk-derived  $A(G)$ ,  $TO(G)$ ,  $LO(G)$ , and  $LA(X)$  modes. However, there exists a significant LO/TO mode mixing for the surface-related  $SO$  mode. This effect persists even in the very small GaP dots; Fig. 6-a shows the bulk TO and LO band parentage of Eq. 12 for the modes of the  $D = 22.2 \text{ \AA}$  dot. Again, we see that significant LO/TO mode mixing exists only in the frequency range where, according to the analysis of the localization radii in Fig. 6-c, the modes are surfacelike.

### IV. SUMMARY

We have developed an atomic-force field for GaP, which gives an accurate bulk-phonon dispersion. This atomistic model is then used to calculate the phonon frequencies and eigenmodes of GaP quantum dots. The resulting several thousands of dot eigenmodes have been analyzed using the projection approach in reciprocal space and the localization radius in real space. We have found that the surface modes can be distinguished from the bulklike modes in both recip-

rocal and real space. In particular, we conclude the following.

1! The *bulklike modes* are localized inside the dot and have a clearly pronounced bulk Brillouin-zone parentage in reciprocal space. The frequencies of these modes can be approximated by the “truncated crystal method” with a single-bulk phonon band at a single-wave vector  $\mathbf{k}^*$ . The bulklike  $G$ -derived  $TO$ - and  $LO$ -phonon dot modes both shift down in frequency with decreasing dot size. Unlike the case in PbS dots,<sup>1</sup> there is almost no LO/TO mixing for the bulklike modes.

2! The *surface modes* are located in the frequency range  $\omega \approx 120 \text{--} 130 \text{ THz}$  between the bulk  $TO$ - and  $LO$ -phonon bands, and in the range  $\omega \approx 60 \text{--} 90 \text{ THz}$  between the bulk  $LA$ - and  $TO$ -phonon bands. These surface modes are localized at the periphery of the dot. Their eigenmodes represent a superposition of many bulk bands with  $\mathbf{k}$  points from all over the bulk Brillouin zone. The surface dot modes in the frequency range  $\omega \approx$